

Facile synthesis of σ,μ -iminoacyl bridged butterfly clusters $(\mu\text{-RE})(\sigma,\mu\text{-ArC=NAr}')\text{Fe}_2(\text{CO})_6$ (E = S, Se)

Chao-Guo Yan ^{a,*}, Jing Sun ^a, Jie Sun ^b

^a Department of Chemistry, Yangzhou University, Yangzhou 225002, PR China

^b Laboratory of Organometallic Chemistry, Shanghai Institute of Organic Chemistry, Shanghai 200032, PR China

Received 3 December 1998; received in revised form 30 March 1999

Abstract

The reactive anionic salts $[\text{Et}_3\text{NH}][(\mu\text{-RE})(\mu\text{-CO})\text{Fe}_2(\text{CO})_6]^-$ (**1**) (RE = PhS, PhSe) reacted with *N*-arylbzimidoyl chloride $\text{Ph}(\text{Cl})\text{C=NAr}'$ (**2**) (Ar = Ph, 4-MeC₆H₄, 4-C₆H₄) in THF to give butterfly σ,μ -iminoacyl bridged hexacarbonyldiiron clusters $(\mu\text{-RE})(\sigma,\mu\text{-PhC=NAr}')\text{Fe}_2(\text{CO})_6$ (**3a–e**) in moderate yields. The structure of the new clusters was characterized by elemental analyses, IR and ¹H-NMR spectroscopy. X-ray diffraction confirmed the crystal structure of $(\mu\text{-PhSe})(\sigma,\mu\text{-PhC=NPh})\text{Fe}_2(\text{CO})_6$ (**3a**). It crystallizes in the triclinic space group *P*1 (no. 2) with $a = 11.224(3)$, $b = 13.542(4)$, $c = 8.9559(2)$ Å, $\alpha = 102.32(2)$, $\beta = 91.95(2)$, $\gamma = 70.20(2)^\circ$, $V = 1250.1(6)$ Å³, $Z = 2$ and $D_{\text{calc}} = 1.636$ g cm⁻³. © 1999 Elsevier Science S.A. All rights reserved.

Keywords: Iminoacyl complex; Carbonyl–iron; Sulfur; Selenium; Crystal structure

1. Introduction

Since Seyferth et al. first reported in 1985 [1], the reactive anion $[(\mu\text{-RS})(\mu\text{-CO})\text{Fe}_2(\text{CO})_6]^-$ and its selenato-analog $[(\mu\text{-RSe})(\mu\text{-CO})\text{Fe}_2(\text{CO})_6]^-$, mainly due to the work of Seyferth et al. [2–4] and Song et al. [5–7], they have become very useful reagents, synthesizing a variety of carbonyl–iron clusters.

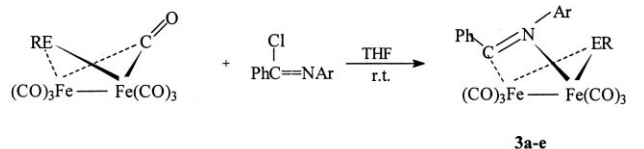
Our ongoing program is aimed at extending their application to synthesize more novel clusters. As a continuation of this project, we further investigated the reactivity of the anions $(\mu\text{-RE})(\mu\text{-CO})\text{Fe}_2(\text{CO})_6$ (E = S, Se) toward an organic electrophile, *N*-arylbzimidoyl chloride. We shall describe here the results of syntheses of *N*-iminoacyl-bridged clusters $(\mu\text{-RE})(\mu\text{-ArC=NAr}')\text{Fe}_2(\text{CO})_6$ from the reactions studied, and X-ray diffraction analysis for a representative cluster $(\mu\text{-PhSe})(\mu\text{-PhC=NPh})\text{Fe}_2(\text{CO})_6$.

2. Results and discussion

The reactive intermediates $[\text{Et}_3\text{NH}][(\mu\text{-PhS})(\mu\text{-CO})\text{Fe}_2(\text{CO})_6]^-$, prepared in situ from $\text{Fe}_3(\text{CO})_{12}$, Et_3N and PhSH reacted smoothly with *N*-arylbzimidoyl chloride (Aryl = phenyl, 4-methylphenyl) to yield the expected μ -iminoacyl bridged clusters **3a** and **3b** (Scheme 1). This type of μ -iminoacyl bridged carbonyl–iron cluster has been synthesized by reaction of triiron dodecarbonyl with thiomidates, or by the reaction of $[\text{Et}_3\text{NH}][(\mu\text{-RS})(\mu\text{-CO})\text{Fe}_2(\text{CO})_6]^-$ (R = alkyl) with *N*-phenylbzimidoyl chloride [8]. The selenato-bridged intermediate $[\text{Et}_3\text{NH}][(\mu\text{-ArSe})(\mu\text{-CO})\text{Fe}_2(\text{CO})_6]^-$ reacts similarly with benzimidoyl chloride to give clusters **3c–e** in moderate yields. Mechanically, the formation of the μ -iminoacyl bridged cluster is apparently a nucleophilic substitution. The iron-centered anion attacks the carbon atom of the benzimidoyl group and eliminates the chloride ion. Then the nitrogen atom coordinates the other iron atom while replacing the $\mu\text{-CO}$ group to complete the reaction.

Clusters **3a–e** have been characterized by elemental analysis, IR and ¹H-NMR spectroscopy, and like **3c**, by

* Corresponding author.



	a	b	c	d	e
RE	PhS	PhS	PhSe	PhSe	PhSe
Ar	Ph	4-MeC ₆ H ₄	Ph	4-MeC ₆ H ₄	4-ClC ₆ H ₄

Scheme 1.

Table 1
Crystal data and refinement for complex **3c**

Empirical formula	C ₂₅ H ₁₅ O ₆ NSeFe ₂
Formula weight	616.05
Crystal system	Triclinic
Space group	<i>P</i> 1 (no. 2)
<i>a</i> (Å)	11.224(3)
<i>b</i> (Å)	13.542(4)
<i>c</i> (Å)	8.9559(2)
α (°)	102.32(2)
β (°)	91.95(2)
γ (°)	70.20(2)
<i>V</i> (Å ³)	1250.1(6)
<i>Z</i>	2
<i>D</i> _{calc} (g cm ⁻³)	1.636
<i>F</i> (000)	612.00
μ (Mo-K α) (cm ⁻¹)	26.55
Temperature (K)	20.0
Scan type	ω -2 θ
Total reflections measured	3641
No. of unique reflections	3392 [<i>R</i> _{int} = 0.018]
Reflections observed [<i>I</i> > 3.00 σ (<i>I</i>)]	2688
No. variables	377
Residuals	<i>R</i> = 0.026, <i>wR</i> = 0.033
Goodness-of-fit indicator	1.90
Max. shift/error in final cycle	0.04
Largest difference peak and hole (e Å ⁻³)	0.30 and -0.36

X-ray diffraction. The IR spectra of **3a–e** showed four to five strong absorption bands in the region of 1950–2100 cm⁻¹, which are the characteristic bands of the terminal carbonyls attached to iron atoms. There is also one medium absorption band at around 1540 cm⁻¹ in the IR spectra of the clusters, which was apparently attributed to the iminoacyl C=N double band. This band is shifted somewhat to a lower frequency when compared to the parent thioimidates ($\nu_{\text{C=N}}$ 1610–1630 cm⁻¹) [8], which is the result of the bridged coordination. The ¹H-NMR spectra of **3a–e** all exhibited the presence of their respective organic groups.

In order to further confirm the structure of such μ -iminoacyl bridged clusters, an X-ray diffraction analysis for **3c** was undertaken. The data collection and processing parameters, atomic coordinate equivalent isotropic thermal parameters, and selected bond lengths and angles are listed in Tables 1 and 2. Fig. 1 shows the

ORTEP representation of the molecule. As seen from Fig. 1, the molecule exhibits a typical butterfly core (Fe₂SeCN) with Fe₂Se and Fe₂CN as two wings. The dihedral angle between the two wing planes is 90.34°. The six-coordinate atoms or groups around each iron atom display as a distorted octahedron. The Fe–Fe distance is 2.5799(8) Å, which is similar to the analogous selenato-bridged cluster 2.544(2) Å in (μ -PhSe)(σ , μ -CH=CHPh)Fe₂(CO)₆ [11], 2.648(3) Å in (μ -PhSe)(μ -PhCH₂SC=S)Fe₂(CO)₆ [9], and the two selenato-bridged clusters 2.601(4), 2.575(4) Å in [(μ -CH₃C₆H₄Se)Fe₂(CO)₆]₂(μ_4 -Se) [10], 2.534 Å in (μ -SePhC=CHSe- μ)Fe₂(CO)₆ [11].

The iminoacyl group is coordinated to Fe(2) via a Fe–C σ -bond (Fe(2)–C(7) 1.982(4) Å, C(7) is in sp² form. The iminoacyl group coordinates to Fe(1) via the donation of an unshared electron pair from the N atom (Fe(1)–N 2.000(3) Å). This represents that the iminoacyl group is in σ , *n* coordinate pattern. There are two possible coordinate patterns for iminoacyl group as in the A (σ , π) and B (σ , *n*) isomers. Since two isomers are structurally very similar, differentiation between them based on the spectroscopic data alone is very difficult. Seyferth suggested that the B-isomer is more consistent with the observed IR spectrum [8]. From the crystal structure we can conclude that the iminoacyl group coordinated to the iron atom with a σ , *n* pattern. The C=N bond length (1.287(4) Å) is identical within experimental error to the values of 1.254(7) and 1.291(7) Å observed for the two independent C=N bonds in (μ -Me₂C=N)(μ -Me₂C=N-O)Fe₂(CO)₆ [12]. This means that the C=N bond in **3c** is a normal bond value and falls in the range 1.24–1.29 Å observed in ordinary organic compounds. The angles of Fe(1)–Se–C(20) and Fe(2)–Se–C(20) are 113.5(1) and 112.2(1)°; this reveals that the phenyl group attached to the Se atom is at an equatorial position, namely **3c** is an *E*-type isomer, which can be seen intuitively from Fig. 1.

Table 2
Selected bond lengths (Å) and angles (°)

Se–Fe(1)	2.3708(8)	Se–Fe(2)	2.3724(8)
Se–C(20)	1.931(4)	Fe(1)–Fe(2)	2.5799(8)
Fe(1)–N	2.000(3)	Fe(1)–C(1)	1.788(4)
Fe(1)–C(2)	1.805(4)	Fe(1)–C(3)	1.791(5)
Fe(2)–C(4)	1.773(5)	Fe(2)–C(5)	1.799(4)
Fe(2)–C(6)	1.811(5)	Fe(2)–C(7)	1.982(4)
N–C(7)	1.287(4)	N–C(14)	1.456(5)
C(7)–C(8)	1.482(5)		
Fe(1)–Se–Fe(2)	65.90(3)	Fe(1)–Se–C(20)	113.5(1)
Fe(2)–Se–C(20)	112.2(1)	Se–Fe(1)–Fe(2)	57.08(2)
Se–Fe(2)–Fe(1)	57.02(2)	Se–Fe(1)–N	79.98(9)
Fe(1)–Fe(2)–N	71.32(9)	Se–Fe(2)–C(7)	80.3(1)
Fe(1)–Fe(2)–C(7)	70.76(10)	Fe(1)–N–C(7)	107.6(2)
Fe(1)–N–C(14)	127.4(2)	C(7)–N–C(14)	124.7(3)
Fe(2)–C(7)–N	110.3(2)	Fe(2)–C(7)–C(8)	125.8(3)
N–C(7)–C(8)	123.7(3)		

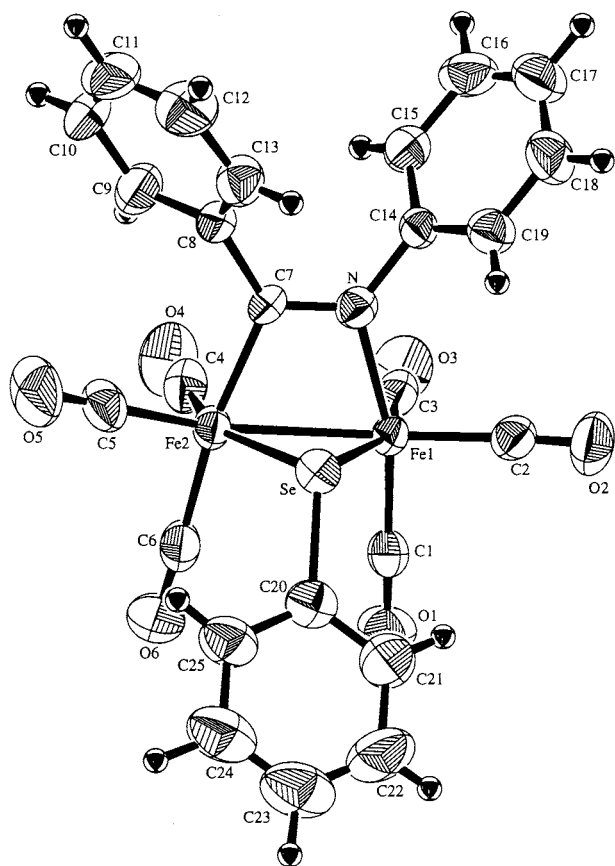


Fig. 1. Molecular structure of cluster **3c**.

3. Experimental

3.1. General

All reactions were carried out under prepurified tank nitrogen using standard Schlenk or vacuum line techniques. THF and diethylether were distilled from sodium benzophenone ketyl, while triethylamine was distilled from potassium hydroxide under nitrogen. Thiophenol was chemically pure. Triiron dodecacarbonyl [13], benzeneselenol [14] and *N*-arylbenzimidoyl chloride $\text{PhC}(\text{Cl})=\text{NAr}$ [15,16] were all prepared according to the literature.

The progress of all reactions was monitored by TLC. Products were purified by column chromatography (30×2.4 cm, 200–300 mesh silica gel) or by TLC ($20 \times 25 \times 0.025$ cm, 10–40 μm silica gel G). The eluents were light petroleum ether (60–90°C) and methylene chloride, used without further purification. All the products were recrystallized from CH_2Cl_2 –hexane and characterized by elemental analysis and IR, $^1\text{H-NMR}$ spectroscopy. Elemental analysis was performed by an Erba 1106 analyzer. IR spectra were recorded on a Nicolet FT-IR 5DX spectrometer with KBr discs. Proton-NMR spectra were recorded on a Bruker 300 spectrometer with a CDCl_3 solvent and a TMS internal standard.

3.2. Reaction of $[\text{Et}_3\text{NH}][(\mu\text{-PhS})(\mu\text{-CO})\text{Fe}_2(\text{CO})_6]$ (**1**) with $\text{Ph}(\text{Cl})\text{C}=\text{NPh}$

A 100 ml three-necked round-bottomed flask equipped with a stir-bar, N_2 inlet tube, and serum caps was charged with 1.00 g (1.98 mmol) of $\text{Fe}_3(\text{CO})_{12}$ and 40 ml of THF. To the resulting green solution were added 0.50 ml (3.00 mmol) of triethylamine and 0.21 ml (2.00 mmol) thiophenol. The mixture was stirred at room temperature (r.t.) for 30 min and the solution turned to red–brown. The resulting $[\text{Et}_3\text{NH}][(\mu\text{-PhS})(\mu\text{-CO})\text{Fe}_2(\text{CO})_6]$ (**1**) reagent solution was cooled to 0°C and added by cannula, 0.65 g (3.00 mmol) *N*-phenylbenzimidoyl chloride dissolved in 15 ml THF. The mixture was stirred at r.t. for 24 h. Solvent was removed under vacuum to leave a red residue, which was extracted with petroleum ether and purified by filtration chromatography, then purified further by TLC using petroleum ether as eluent. The first red band gave 0.237 g (24%) of $(\mu\text{-PhS})_2\text{Fe}_2(\text{CO})_6$, which was identified by comparison of its melting point and $^1\text{H-NMR}$ spectrum with those given in the literature [17]. The second red band gave 0.350 g (31%) of $(\mu\text{-PhS})(\sigma,\mu\text{-PhC}=\text{NPh})\text{Fe}_2(\text{CO})_6$ (**3a**) as a red solid. M.p. (dec.) 158–160°C. Anal. Calc. for $\text{C}_{25}\text{H}_{15}\text{Fe}_2\text{NO}_6\text{S}$: C, 52.76; H, 2.66. Found: C, 52.38; H, 2.94%. $^1\text{H-NMR}$ (CDCl_3): δ 6.60–7.60 (3 C_6H_5) ppm. IR (KBr disc): ν 2071(s), 2022(vs), 1992(vs), 1978(vs), 1945(s) ($\text{C}=\text{O}$), 1535(m) ($\text{C}=\text{N}$) cm^{-1} .

3.3. Reaction of $[\text{Et}_3\text{NH}][(\mu\text{-PhS})(\mu\text{-CO})\text{Fe}_2(\text{CO})_6]$ (**1**) with $\text{Ph}(\text{Cl})\text{C}=\text{NC}_6\text{H}_4\text{CH}_3\text{-}p$

The same procedure as for **3a** was followed, but 0.690 g (3.00 mmol) of $\text{Ph}(\text{Cl})\text{C}=\text{NC}_6\text{H}_4\text{CH}_3\text{-}p$ was used instead of $\text{Ph}(\text{Cl})\text{C}=\text{NPh}$. The first red band gave 0.219 g (22%) of $(\mu\text{-PhS})_2\text{Fe}_2(\text{CO})_6$, which was identified by comparison of its melting point and $^1\text{H-NMR}$ spectrum with those given in the literature. The second red band gave 0.410 g (35%) of $(\mu\text{-PhS})(\sigma,\mu\text{-PhC}=\text{NC}_6\text{H}_4\text{CH}_3\text{-}p)\text{Fe}_2(\text{CO})_6$ (**3b**) as a red solid. M.p. (dec.) 146–148°C. Anal. Calc. for $\text{C}_{26}\text{H}_{17}\text{Fe}_2\text{NO}_6\text{S}$: C, 51.55; H, 2.94. Found: C, 51.69; H, 2.80%. $^1\text{H-NMR}$ (CDCl_3): δ 2.15 (s, 3H, CH_3), 6.61, 7.60 (d, d, $J = 7.0$ Hz, 2H, 2H, C_6H_4), 6.89–7.39 (2 C_6H_5) ppm. IR (KBr disc): ν 2071(vs), 2022(vs), 1993(vs), 1978(vs), 1946(s) ($\text{C}=\text{O}$), 1535(m) ($\text{C}=\text{N}$) cm^{-1} .

3.4. Reaction of $[\text{Et}_3\text{NH}][(\mu\text{-PhSe})(\mu\text{-CO})\text{Fe}_2(\text{CO})_6]$ (**1**) with $\text{Ph}(\text{Cl})\text{C}=\text{NPh}$

A 100 ml three-necked round-bottomed flask equipped with a stir-bar, N_2 inlet tube, and serum caps was charged with 1.00 g (1.98 mmol) of $\text{Fe}_3(\text{CO})_{12}$ and 40 ml of THF. To the resulting green solution were added 0.50 ml (3.00

mmol) of triethylamine and 0.21 ml (2.00 mmol) benzeneselenol. The mixture was stirred at r.t. for 30 min and the solution turned to red–brown. The resulting $[\text{Et}_3\text{NH}][(\mu\text{-PhSe})(\mu\text{-CO})\text{Fe}_2(\text{CO})_6]$ (**1**) reagent solution was cooled to 0°C and added by cannula 0.65 g (3.00 mmol) *N*-phenylbenzimidoyl chloride dissolved in a separate flask in 15 ml THF. The mixture was stirred at r.t. for 24 h. The solvent was removed under vacuum to leave a red residue, which was extracted with petroleum ether and purified by filtration chromatography, then purified further by TLC using petroleum ether as eluent. The first red band gave 0.271 g (23%) of $(\mu\text{-PhSe})_2\text{Fe}_2(\text{CO})_6$, which was identified by comparison of its melting point and $^1\text{H-NMR}$ spectrum with those given in the literature [5]. The second red band gave 0.347 g (28%) of $(\mu\text{-PhSe})(\sigma,\mu\text{-PhC=NPh})\text{Fe}_2(\text{CO})_6$ (**3c**) as a red solid. M.p. (dec.) 140–141°C. Anal. Calc. for $\text{C}_{25}\text{H}_{15}\text{Fe}_2\text{NO}_6\text{Se}$: C, 48.74; H, 2.45. Found: C, 48.44; H, 2.76%. $^1\text{H-NMR}$ (CDCl_3): δ 6.55–7.70 (3 C_6H_5) ppm. IR (KBr, disc): ν 2069(s), 2021(vs), 1991(vs), 1975(vs), 1950(s) (C=O), 1530(m) (C=N) cm^{-1} .

3.5. Reaction of $[\text{Et}_3\text{NH}][(\mu\text{-PhSe})(\mu\text{-CO})\text{Fe}_2(\text{CO})_6]$ (**1**) with $\text{Ph}(\text{Cl})\text{C=NC}_6\text{H}_5\text{CH}_3\text{-}p$

The same procedure as for **3c** was followed, but 0.690 g (3.00 mmol) of $\text{Ph}(\text{Cl})\text{C=NC}_6\text{H}_4\text{CH}_3\text{-}p$ was used instead of $\text{Ph}(\text{Cl})\text{C=NPh}$. The first red band gave 0.209 g (18%) of $(\mu\text{-PhSe})_2\text{Fe}_2(\text{CO})_6$, which was identified by comparison of its melting point and $^1\text{H-NMR}$ spectrum with those given in the literature [5]. The second red band gave 0.350 g (28%) of $(\mu\text{-PhSe})(\sigma,\mu\text{-PhC=NC}_6\text{H}_4\text{CH}_3\text{-}p)\text{Fe}_2(\text{CO})_6$ (**3d**) as a red solid. M.p. (dec.) 142–144°C. Anal. Calc. for $\text{C}_{26}\text{H}_{17}\text{Fe}_2\text{NO}_6\text{Se}$: C, 49.56; H, 2.72. Found: C, 50.02; H, 3.04%. $^1\text{H-NMR}$ (CDCl_3): δ 2.13 (s, 3H, CH_3), 6.74, 7.38 (d, d, $J = 7.0$ Hz, 2H, 2H, C_6H_4), 6.89–7.37 (2 C_6H_5) ppm. IR (KBr, disc): ν 2069(vs), 2020(vs), 1991(vs), 1975(vs), 1944(s) (C=O), 1535(m) (C=N) cm^{-1} .

3.6. Reaction of $[\text{Et}_3\text{NH}][(\mu\text{-PhSe})(\mu\text{-CO})\text{Fe}_2(\text{CO})_6]$ (**1**) with $\text{Ph}(\text{Cl})\text{C=NC}_6\text{H}_5\text{Cl-}p$

The same procedure as for **3c** was followed, but 0.615 g (3.00 mmol) of $\text{Ph}(\text{Cl})\text{C=NC}_6\text{H}_4\text{Cl-}p$ was used instead of $\text{Ph}(\text{Cl})\text{C=NPh}$. The first red band gave 0.313 g (26%) of $(\mu\text{-PhSe})_2\text{Fe}_2(\text{CO})_6$, which was identified by comparison of its melting point and $^1\text{H-NMR}$ spectrum with those given in the literature. The second red band gave 0.514 g (40%) of $(\mu\text{-PhSe})(\sigma,\mu\text{-PhC=NC}_6\text{H}_4\text{Cl-}p)\text{Fe}_2(\text{CO})_6$ (**3e**) as a red solid. M.p. (dec.) 124–126°C. Anal. Calc. for $\text{C}_{25}\text{H}_{15}\text{ClFe}_2\text{NO}_6\text{S}$: C, 46.16; H, 2.17. Found: C, 46.35; H, 2.56%. $^1\text{H-NMR}$ (CDCl_3): δ 6.53–7.53 (2 C_6H_5 , C_6H_4) ppm. IR (KBr, disc): ν 2067(vs), 2020(vs), 1992(vs), 1978(vs), 1945(s) (C=O), 1540(m) (C=N) cm^{-1} .

3.7. Crystal structure determination of **3c**

A red prismatic crystal of $\text{C}_{25}\text{H}_{15}\text{O}_6\text{NSeFe}_2$ having approximate dimensions of $0.20 \times 0.20 \times 0.30$ mm was mounted on a glass fiber. All measurements were made on a Rigaku AFC7R diffractometer with graphite monochromated Mo-K_α radiation and a 12 kW rotating anode generator. Cell constants and an orientation matrix for data collection, obtained from a least-squares refinement using the setting angles of 18 carefully centered reflections in the range $18.333^\circ < 2\theta < 24.42^\circ$ corresponded to a primitive triclinic cell. The data were collected at a temperature of $20 \pm 1^\circ\text{C}$ using the $\omega - 2\theta$ scan technique to a maximum 2θ value of 50.0° . ω scans of several intense reflections, made prior to data collection, had an average width at half-height of 0.10 with a take-off angle of 6.0° . Scans of $(1.21 + 0.30 \tan \theta)$ were made at a speed of 16.0 min^{-1} (in ω). The weak reflections [$I < 13.0\sigma(I)$] were rescanned (maximum of four scans) and the counts were accumulated to ensure good counting statistics. Stationary background counts were recorded on each side of the reflection. The ratio of peak counting time to background counting time was 2:1. The diameter of the incident beam collimator was 1.0 mm, the crystal to detector distance was 235 mm, and the computer controlled detector aperture was to 9.0×13.0 mm (horizontal \times vertical). Of the 3641 reflections that were collected, 3392 were unique [$R_{\text{int}} = 0.018$]. The intensities of three representative reflection were measured after every 200 reflections. Over the course of data collection, the standards decreased by -1.1% . A linear correction factor was applied to the data to account for this phenomenon. The linear absorption coefficient μ for Mo-K_α radiation is 26.6 cm^{-1} . An empirical absorption correction based on azimuthal scans of several reflections was applied which resulted in transmission factors ranging from 0.58 to 1.00. The data were corrected for Lorentz and polarization effects. A correction for secondary extinction was applied where the coefficient = $2.433296\text{e-}06$.

The structure was solved by direct methods and expanded using Fourier techniques. The non-hydrogen atoms were refined anisotropically. Hydrogen atoms were refined isotropically. The final cycle of full-matrix least-squares refinement was based on 2688 observed reflections [$I > 3.00\sigma(I)$] and 377 variable parameters and converged (largest parameter was 0.04 times its estimated S.D.) with unweighted and weighted agreement factors of $R = 0.026$, $R_w = 0.033$. The standard deviation of an observation of unit weight [$\Sigma w(|F_o| - |F_c|)/(N_o - N_v)^{1/2} = 1.29$ (N_o = number of observations, N_v = number of variables)]. The weighting scheme was based on counting statistics and included a factor ($p = 0.030$) to downweight the intense reflections. Plots of $\Sigma w(|F_o| - |F_c|)$ versus $|F_o|$, reflection order in data col-

lection, $\sin \theta/\lambda$ and various classes of indices showed no unusual trends. The maximum and minimum peaks on the final difference Fourier map corresponded to 0.30 and -0.36 e \AA^{-3} , respectively. Neutral atom scattering factors were taken from Cromer and Waber [18]. Anomalous dispersion effects were included in F_{calc} [19]; the values for $\Delta f'$ and $\Delta f''$ were those of Creagh and McAuley [20]. The values for the mass attenuation coefficients are those of Creagh and Hubbell [21]. All calculations were performed using the texsan crystallographic software package from the Molecular Structure Corporation.

4. Supplementary material

Further details of the crystal structure investigation may be obtained from the Fachinformationszentrum Karlsruhe, D-76344 Eggenstein-Leopoldshafen, Germany, on quoting the depository number CSD-410428.

Acknowledgements

The authors would like to thank the State Key Laboratory of Organometallic Chemistry at Shanghai Institute of Organic Chemistry for financial support of this work.

References

- [1] D. Seyferth, G.B. Womack, J.C. Dewan, *Organometallics* 4 (1985) 398.
- [2] D. Seyferth, G.B. Womack, C.M. Archer, J.C. Dewan, *Organometallics* 8 (1989) 430.
- [3] D. Seyferth, L.L. Anderson, W.M. Davis, *J. Organomet. Chem.* 459 (1993) 271.
- [4] D. Seyferth, D.P. Ruschke, W.M. Davis, M. Cowie, A.D. Hunter, *Organometallics* 13 (1994) 3834.
- [5] L.-C. Song, C.-G. Yan, Q.-M. Hu, *Acta Chim. Sin.* 53 (1995) 402.
- [6] L.-C. Song, C.-G. Yan, Q.-M. Hu, R.-J. Wang, T.C.W. Mak, X.-Y. Huang, *Organometallics* 15 (1996) 1535.
- [7] L.-C. Song, C.-G. Yan, Q.-M. Hu, B.-M. Wu, T.C.W. Mak, *Organometallics* 16 (1997) 632.
- [8] D. Seyferth, J.B. Hoke, *Organometallics* 7 (1988) 524.
- [9] L.-C. Song, C.-G. Yan, Q.-M. Hu, R.-J. Wang, T.C.W. Mak, *Organometallics* 14 (1995) 5513.
- [10] L.-C. Song, Q.M. Hu, C.-G. Yan, R.J. Wang, T.C.W. Mak, *Acta Crystallogr. C* 52 (1996) 1357.
- [11] P. Mathur, M.M. Hossain, K. Das, U.C. Sinha, *J. Chem. Soc. Chem. Commun.* (1993) 46.
- [12] G.P. Khare, R.J. Doedens, *Inorg. Chem.* 15 (1976) 86.
- [13] R.B. King, *Organic Syntheses*, vol. 1, Academic Press, New York, 1965, p. 95.
- [14] D.G. Foster, *Organic Syntheses*, vol. III, Wiley, New York, 1955, p. 771.
- [15] G.H. Coleman, R.E. Pyle, *J. Am. Chem. Soc.* 68 (1946) 2007.
- [16] W.R. Vaughan, R.D. Carlson, *J. Am. Chem. Soc.* 84 (1962) 769.
- [17] N.S. Nametkin, V.D. Tyurin, M.A. Kukina, *J. Organomet. Chem.* 149 (1978) 355.
- [18] D.T. Cromer, J.T. Waber, *International Tables for X-ray Crystallography*, vol. IV, Kynoch Press, Birmingham, UK, 1974, Table 2.2A.
- [19] J.A. Ibers, W.C. Hamilton, *Acta Crystallogr.* 17 (1964) 781.
- [20] D.C. Creagh, W.J. McAuley, in: A.J.C. Wilson (Ed.), *International Tables for Crystallography*, vol. C, Kluwer, Boston, 1992, Table 4.2.6.8, pp. 219–222.
- [21] D.C. Creagh, J.H. Hubbell, in: A.J.C. Wilson (Ed.), *International Tables for Crystallography*, vol. C, Kluwer, Boston, 1992, Table 4.2.4.3, pp. 200–206.